PAPER

Joint Tx/Rx MMSE Filtering for Single-Carrier MIMO Transmission

Shinya KUMAGAI[†a)], ***Student Member***, **Tatsunori OBARA**[†], **Tetsuya YAMAMOTO**[†], ***Members***, *and* **Fumiyuki ADACHI**[†], ***Fellow***

SUMMARY In this paper, we propose a joint transmit and receive linear filtering based on minimum mean square error criterion (joint Tx/Rx MMSE filtering) for single-carrier (SC) multiple-input multiple-output (MIMO) transmission. Joint Tx/Rx MMSE filtering transforms the MIMO channel to the orthogonal eigenmodes to avoid the inter-antenna interference (IAI) and performs MMSE based transmit power allocation to sufficiently suppress the inter-symbol interference (ISI) resulting from the severe frequency-selectivity of the channel. Rank adaptation and adaptive modulation are jointly introduced to narrow the gap of received signal-to-interference plus noise power ratio (SINR) among eigenmodes. The superiority of the SC-MIMO transmission with joint Tx/Rx MMSE filtering and joint rank adaptation/adaptive modulation is confirmed by computer simulation.
key words: *single-carrier transmission, MIMO, MMSE filtering, rank adaptation, adaptive modulation*

1. Introduction

Multiple-input multiple-output (MIMO) [1] is a powerful technique to increase the transmission data rate by increasing the spatial multiplexing order (i.e., increasing the rank) or to improve the transmission quality by increasing the diversity order (i.e., decreasing the rank). MIMO with orthogonal frequency-division multiplexing (OFDM) [2], [3] is known for its robustness against frequency-selective fading [4]. However, the disadvantage of OFDM is its high peak-to-average power ratio (PAPR) [3], [5].

Recently, MIMO with single-carrier (SC) block transmission [6]–[8] has been attracting much attention as an alternative technique because of its low PAPR property [7]. SC-MIMO suffers not only from the inter-antenna interference (IAI) caused by MIMO multiplexing but also from the inter-symbol interference (ISI) caused by severe frequency-selectivity of the channel. The minimum mean square error based receive linear filtering (Rx MMSE filtering) [6], [7] achieves good transmission performance with low-complexity. However, its performance improvement is limited due to the existence of residual IAI and ISI after MMSE filtering. To improve the transmission performance, non-linear signal detection techniques such as iterative interference cancellation [7] and maximum likelihood based detection [8] were proposed. However, their computation complexity is extremely high.

Another interesting technique to improve the transmission performance is joint transmit/receive linear signal detection [9], [10]. If the channel state information (CSI) of broadband MIMO channel is available at both the transmitter and receiver, the transmission performance can be improved while keeping the computation complexity low. In [9], MMSE based linear precoder and decoder were proposed for MIMO transmission. The optimal precoder and decoder transform the MIMO channel to orthogonal subchannels (i.e., eigenmodes) to avoid the IAI. However, the precoder and decoder are designed for frequency-nonselective MIMO channel only, and therefore, do not consider the ISI. On the other hand, in [10], joint transmit and receive MMSE based frequency-domain equalization (joint Tx/Rx MMSE-FDE) was proposed for SC block transmission. By performing MMSE based transmit power allocation across frequencies, joint Tx/Rx MMSE-FDE sufficiently suppresses the ISI and achieves a better performance than Rx MMSE-FDE [11] which uses the CSI at the receiver only. However, it was designed for single-input single-output (SISO) case only, and therefore, does not consider the IAI.

In this paper, we propose a joint Tx/Rx MMSE based linear filtering for SC-MIMO transmission to suppress both IAI and ISI. The proposed joint Tx/Rx MMSE filtering transforms the MIMO channel to eigenmodes to avoid the IAI and jointly performs MMSE based frequency-domain transmit power allocation and receive FDE on the eigenmodes to suppress the ISI. However, the existence of eigenmodes having low received signal-to-interference plus noise power ratio (SINR) limits the improvement of transmission performance. Therefore, rank adaptation [12] and adaptive modulation [13], [14] are jointly introduced to narrow the gap of received SINR among eigenmodes. The optimal combination of the number of data streams (i.e., rank) and modulation levels is determined based on the minimum bit error rate (BER) criterion.

The remainder of this paper is organized as follows. Section 2 presents the transmission system model and signal representation for SC-MIMO transmission with joint Tx/Rx MMSE filtering and joint rank adaptation/adaptive modulation and then, presents the derivation of optimal Tx/Rx filters. Section 3 describes joint rank adaptation/adaptive modulation. In Sect. 4, we evaluate the BER performance achievable with the SC-MIMO transmission using joint

Manuscript received December 19, 2013.
Manuscript revised May 13, 2014.
[†]The authors are with the Department of Communications Engineering, Graduate School of Engineering, Tohoku University, Sendai-shi, 980-8579 Japan.
a) E-mail: kumagai@mobile.ecei.tohoku.ac.jp
DOI: 10.1587/transcom.E97.B.1967

Tx/Rx MMSE filtering and joint rank adaptation/adaptive modulation by computer simulation. Section 5 gives the concluding remarks.

2. SC-MIMO Transmission with Joint Tx/Rx MMSE Filtering and Joint Rank Adaptation/Adaptive Modulation

2.1 System Model and Signal Representation

A system model of SC-MIMO transmission with joint Tx/Rx MMSE filtering and joint rank adaptation/adaptive modulation is illustrated in Fig. 1. A transmitter and a receiver have N_t and N_r antennas, respectively. The information bit sequence is data modulated based on the joint rank adaptation/adaptive modulation described in Sect. 3 to G (less than or equal to min(N_t,N_r)) parallel streams of N_c-symbol blocks, where N_c is the size of discrete Fourier transform (DFT) and inverse DFT (IDFT). The symbol block of each stream is transformed into a frequency-domain signal by N_c-point DFT.

The $N_t \times 1$ transmit symbol vector $\mathbf{S}(k)$ at the k $(= 0 \sim N_c - 1)$th frequency is obtained by applying the Tx MMSE filtering to the $N_t \times 1$ frequency-domain signal vector $\mathbf{D}(k) = [D_0(k), \ldots, D_g(k), \ldots, D_{G-1}(k)]^T$ after N_c-point DFT, which is expressed as

$$\begin{aligned}\mathbf{S}(k) &= [S_0(k), \ldots, S_n(k), \ldots, S_{N_t-1}(k)]^T \\ &= \mathbf{W}_t(k)\mathbf{D}(k),\end{aligned} \tag{1}$$

where $(.)^T$ is the transpose operation and $\mathbf{W}_t(k)$ is the $N_t \times G$ Tx filter matrix. N_c-point IDFT is applied to each transmit symbol block $\{S_n(k); k = 0 \sim N_c - 1\}$, $n = 0 \sim N_t - 1$. Finally, the last N_g symbols of each transmit block are copied as a cyclic prefix (CP) and inserted into the guard interval (GI) at the beginning of each block before transmission.

At the receiver, after removing CP, the superimposed signal block received by each of N_r antennas is transformed into the frequency-domain signal byN_c-point DFT. The $N_r \times 1$ frequency-domain received signal vector $\mathbf{R}(k)$ at the kth frequency after N_c-point DFT is expressed as

$$\begin{aligned}\mathbf{R}(k) &= [R_0(k), \ldots, R_m(k), \ldots, R_{N_r-1}(k)]^T \\ &= \sqrt{\frac{2E_s}{T_s}}\mathbf{H}(k)\mathbf{S}(k) + \mathbf{Z}(k),\end{aligned} \tag{2}$$

where E_s and T_s are the average transmit symbol energy and symbol duration, respectively. $\mathbf{H}(k)$ is the $N_r \times N_t$ MIMO channel matrix and $\mathbf{Z}(k) = [Z_0(k), \ldots, Z_m(k), \ldots, Z_{N_r-1}(k)]^T$ is the noise vector whose elements are zero-mean complex-valued random variables having the identical variance $2N_0/T_s$ with N_0 being the one-sided power spectrum density of additive white Gaussian noise (AWGN).

The $G \times 1$ frequency-domain soft-output vector $\hat{\mathbf{D}}(k)$ is obtained by performing the Rx MMSE filtering on $\mathbf{R}(k)$ as

$$\begin{aligned}\hat{\mathbf{D}}(k) &= \left[\hat{D}_0(k), \ldots, \hat{D}_g(k), \ldots, \hat{D}_{G-1}(k)\right]^T \\ &= \mathbf{W}_r(k)\mathbf{R}(k) \\ &= \sqrt{\frac{2E_s}{T_s}}\mathbf{W}_r(k)\mathbf{H}(k)\mathbf{W}_t(k)\mathbf{D}(k) + \mathbf{W}_r(k)\mathbf{Z}(k),\end{aligned} \tag{3}$$

where $\mathbf{W}_r(k)$ is the $G \times N_r$ Rx filter matrix. N_c-point IDFT is applied to each frequency-domain soft-output block $\{\hat{D}_g(k); k = 0 \sim N_c - 1\}$, $g = 0 \sim G - 1$, and then the G parallel time-domain soft-output blocks are obtained.

2.2 Derivation of Tx/Rx Filters

In this section, we derive the optimal transmit and receive filters based on MMSE criterion. The total MSE ε of the blocks between the transmit symbol vector $\mathbf{D}(k)$ and the soft-output vector $\hat{\mathbf{D}}(k)$ is defined as

$$\varepsilon \equiv E\left[\sum_{k=0}^{N_c-1}\mathrm{tr}\left\{\left(\mathbf{D}(k) - \frac{\hat{\mathbf{D}}(k)}{\sqrt{\frac{2E_s}{T_s}}}\right)\left(\mathbf{D}(k) - \frac{\hat{\mathbf{D}}(k)}{\sqrt{\frac{2E_s}{T_s}}}\right)^H\right\}\right], \tag{4}$$

where $E(.)$, tr(.), and $(.)^H$ are the ensemble average operation, trace operation, and Hermitian transpose operation, respectively. Substituting Eq. (3) into Eq. (4), the total MSE can be rewritten as

$$\begin{aligned}\varepsilon = &\sum_{k=0}^{N_c-1}\mathrm{tr}\left\{\begin{array}{l}(\mathbf{I}_G - \mathbf{W}_r(k)\mathbf{H}(k)\mathbf{W}_t(k)) \\ \times(\mathbf{I}_G - \mathbf{W}_r(k)\mathbf{H}(k)\mathbf{W}_t(k))^H\end{array}\right\} \\ &+ \gamma^{-1}\sum_{k=0}^{N_c-1}\mathrm{tr}\left\{\mathbf{W}_r(k)\mathbf{W}_r^H(k)\right\},\end{aligned} \tag{5}$$

where $\mathbf{I}_A$ is the $A \times A$ identity matrix and $\gamma = E_s/N_0$. Here, we use $E[\mathbf{D}(k)\mathbf{D}^H(k)] = \mathbf{I}_G$ and $E[\mathbf{Z}(k)\mathbf{Z}^H(k)] = (2N_0/T_s)\mathbf{I}_{N_r}$. The minimization of the total MSE ε under

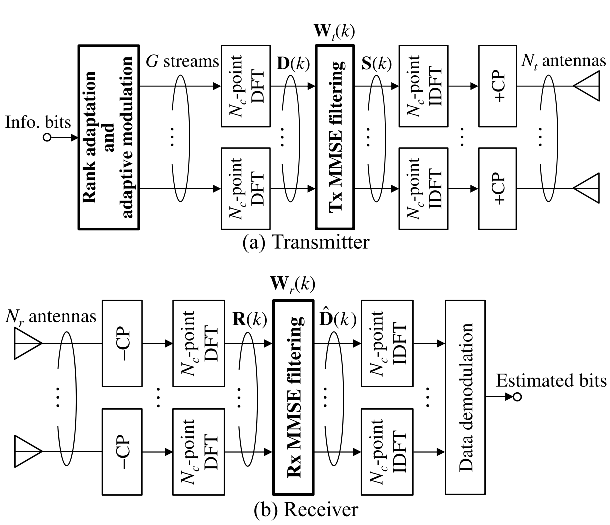

Fig. 1 SC-MIMO transmission with joint Tx/Rx MMSE filtering and joint rank adaptation/adaptive modulation.

the total transmit power constraint is an optimization problem given as

$$\left\{\mathbf{W}_{t,opt}(k), \mathbf{W}_{r,opt}(k)\right\} = \underset{\{\mathbf{W}_t(k),\mathbf{W}_r(k);k=0\sim N_c-1\}}{\arg\min} \varepsilon \quad \text{s.t.} \sum_{k=0}^{N_c-1} \mathrm{tr}\left\{\mathbf{W}_t(k)\mathbf{W}_t^H(k)\right\} = N_c. \tag{6}$$

The Tx and Rx filters which satisfy Eq. (6) are the MMSE solution. However, it is quite difficult to derive a set of MMSE filter matrices $\left\{\mathbf{W}_{t,opt}(k), \mathbf{W}_{r,opt}(k)\right\}$ at the same time since $\mathbf{W}_t(k)$ is the function of $\mathbf{W}_r(k)$ or vice versa. Therefore, in this paper, as in [10], we consider the concatenation of Tx filter and MIMO channel as a equivalent channel $\overline{\mathbf{H}}(k) = \mathbf{H}(k)\mathbf{W}_t(k)$ and first, we derive the optimal Rx filter matrix $\mathbf{W}_{r,opt}(k)$. Then, we derive the optimal Tx filter matrix $\mathbf{W}_{t,opt}(k)$ by solving the optimization problem of Eq. (6) for the given $\mathbf{W}_{r,opt}(k)$.

The objective function given as Eq. (5) is a convex function because the Hessian matrix $\nabla^2\varepsilon$ is positive semidefinite [15]. Therefore, the objective function is minimized when $\partial\varepsilon/\partial\mathbf{W}_r(k) = 0$. As a consequence, $\mathbf{W}_{r,opt}(k)$ is obtained as

$$\mathbf{W}_{r,opt}(k) = \overline{\mathbf{H}}^H(k)\left\{\overline{\mathbf{H}}(k)\overline{\mathbf{H}}^H(k) + \gamma^{-1}\mathbf{I}_{N_r}\right\}^{-1}. \tag{7}$$

Substituting Eq. (7) into Eq. (6) and using the matrix inversion lemma [16], the optimization problem is rewritten as

$$\begin{aligned}&\mathbf{W}_{t,opt}(k)\\ &= \underset{\{\mathbf{W}_t(k);k=0\sim N_c-1\}}{\arg\min} \sum_{k=0}^{N_c-1} \mathrm{tr}\left\{\begin{array}{l}\gamma\mathbf{H}(k)\mathbf{W}_t(k)\\ \times \mathbf{W}_t^H(k)\mathbf{H}^H(k) + \mathbf{I}_{N_r}\end{array}\right\}^{-1}\\ &\text{s.t.} \sum_{k=0}^{N_c-1} \mathrm{tr}\left\{\mathbf{W}_t(k)\mathbf{W}_t^H(k)\right\} = N_c.\end{aligned} \tag{8}$$

For any $I \times I$ square matrix $\mathbf{A}$, it is true that $\mathrm{tr}[\mathbf{A}] = \sum_{i=0}^{I-1} \lambda_i$, where λ_i is the i $(= 0 \sim I-1)$th eigenvalue of $\mathbf{A}$ [16]. Therefore, Eq. (8) can be rewritten as

$$\begin{aligned}&\mathbf{W}_{t,opt}(k)\\ &= \underset{\{\mathbf{W}_t(k);k=0\sim N_c-1\}}{\arg\min} \sum_{k=0}^{N_c-1} \mathrm{tr}\left\{\begin{array}{l}\gamma\mathbf{H}(k)\mathbf{W}_t(k)\\ \times \mathbf{W}_t^H(k)\mathbf{H}^H(k) + \mathbf{I}_{N_r}\end{array}\right\}^{-1}\\ &= \underset{\{\mathbf{W}_t(k);k=0\sim N_c-1\}}{\arg\min} \sum_{k=0}^{N_c-1} \mathrm{tr}\left\{\begin{array}{l}\gamma\mathbf{W}_t(k)\mathbf{W}_t^H(k)\\ \times \mathbf{H}^H(k)\mathbf{H}(k) + \mathbf{I}_{N_t}\end{array}\right\}^{-1}\\ &= \underset{\{P_g(k);g=0\sim G-1,k=0\sim N_c-1\}}{\arg\min} \sum_{k=0}^{N_c-1}\sum_{g=0}^{G-1}\left\{\gamma P_g(k)\Lambda_g(k) + 1\right\}^{-1}\\ &\text{s.t.} \sum_{k=0}^{N_c-1} \mathrm{tr}\left\{\mathbf{W}_t(k)\mathbf{W}_t^H(k)\right\} = N_c.\end{aligned} \tag{9}$$

Here, we use $\mathrm{tr}[\mathbf{AB}] = \mathrm{tr}[\mathbf{BA}]$, where $\mathbf{A}$ and $\mathbf{B}$ are respectively $A \times B$ and $B \times A$ matrices. $P_g(k)$ and $\Lambda_g(k)$ are the gth eigenvalue of $\mathbf{W}_t(k)\mathbf{W}_t^H(k)$ and $\mathbf{H}^H(k)\mathbf{H}(k)$, respectively.

$\mathbf{H}(k)$ and $\mathbf{W}_t(k)$ can be transformed by singular value decomposition [16] as

$$\begin{cases}\mathbf{H}(k) = \mathbf{U}_h(k)\sqrt{\mathbf{\Lambda}(k)}\mathbf{V}_h^H(k)\\ \mathbf{W}_t(k) = \mathbf{U}_t(k)\sqrt{\mathbf{P}(k)}\mathbf{V}_t^H(k)\end{cases}, \tag{10}$$

where $\mathbf{V}_h(k)$ and $\mathbf{U}_t(k)$ are respectively the $N_t \times N_t$ unitary matrices. $\mathbf{U}_h(k)$ is the $N_r \times N_r$ unitary matrix and $\mathbf{V}_t(k)$ is the $G \times G$ unitary matrix. $\mathbf{\Lambda}(k)$ is the $N_r \times N_t$ matrix whose (i,i)th element is $\Lambda_i(k); i = 0 \sim \mathrm{rank}[\mathbf{H}^H(k)\mathbf{H}(k)]$, and any other elements are zero. $\mathbf{P}(k)$ is the $N_t \times G$ matrix whose (g,g)th element is $P_g(k)$ and any other elements are zero. Therefore Eq. (8) can also be rewritten by substituting Eq. (10) as

$$\begin{aligned}&\mathbf{W}_{t,opt}(k)\\ &= \underset{\{\mathbf{P}(k),\mathbf{U}_t(k);k=0\sim N_c-1\}}{\arg\min} \sum_{k=0}^{N_c-1} \mathrm{tr}\left\{\begin{array}{l}\gamma\sqrt{\mathbf{\Lambda}(k)}\mathbf{V}_h^H(k)\mathbf{U}_t(k)\\ \times\sqrt{\mathbf{P}(k)}\sqrt{\mathbf{P}^T(k)}\mathbf{U}_t^H(k)\\ \times\mathbf{V}_h(k)\sqrt{\mathbf{\Lambda}^T(k)} + \mathbf{I}_{N_r}\end{array}\right\}^{-1}\\ &\text{s.t.} \sum_{k=0}^{N_c-1} \mathrm{tr}\left\{\sqrt{\mathbf{P}(k)}\sqrt{\mathbf{P}^T(k)}\right\} = N_c.\end{aligned} \tag{11}$$

Since Eq. (11) is equal to Eq. (9), $\mathbf{U}_t(k) = \mathbf{V}_h(k)$. Furthermore, $\mathbf{V}_t(k)$ does not appear in Eq. (11). Therefore, the optimization problem does not depend on $\mathbf{V}_t(k)$. Accordingly, $\mathbf{V}_t(k)$ can be set to an arbitrary $G \times G$ unitary matrix for all k. In this paper, we set $\mathbf{V}_{t,opt}(k) = \mathbf{I}_G$ for the sake of brevity (the impact of $\mathbf{V}_t(k)$ on the PAPR of the transmit signal is discussed in Appendix A.). As a consequence, $\mathbf{W}_{t,opt}(k)$ is expressed as

$$\mathbf{W}_{t,opt}(k) = \mathbf{V}_h(k)\sqrt{\mathbf{P}_{opt}(k)}. \tag{12}$$

The optimization problem is rewritten by substituting Eq. (12) into Eq. (11) as

$$\begin{aligned}&P_{g,opt}(k)\\ &= \underset{\{P_g(k);g=0\sim G-1,k=0\sim N_c-1\}}{\arg\min} \sum_{k=0}^{N_c-1}\sum_{g=0}^{G-1}\frac{1}{\gamma P_g(k)\Lambda_g(k)+1}\\ &\text{s.t.} \begin{cases}\sum_{k=0}^{N_c-1}\sum_{g=0}^{G-1} P_g(k) = N_c\\ P_g(k)\geq 0 \text{ for } g=0\sim G-1 \text{ and } k=0\sim N_c-1,\end{cases}\end{aligned} \tag{13}$$

which can be solved by non-linear programming and the solution satisfies Karush-Kuhn-Tucker (KKT) condition [15]. Following [15], the optimal solution is given as (the derivation is shown in Appendix B)

$$P_{g,opt}(k) = \max\left\{\frac{1}{\sqrt{\mu}}\frac{1}{\sqrt{\gamma\Lambda_g(k)}} - \frac{1}{\gamma\Lambda_g(k)}, 0\right\}, \tag{14}$$

where μ is chosen to satisfy the constraint condition in Eq. (13) (i.e., total transmit power constraint).

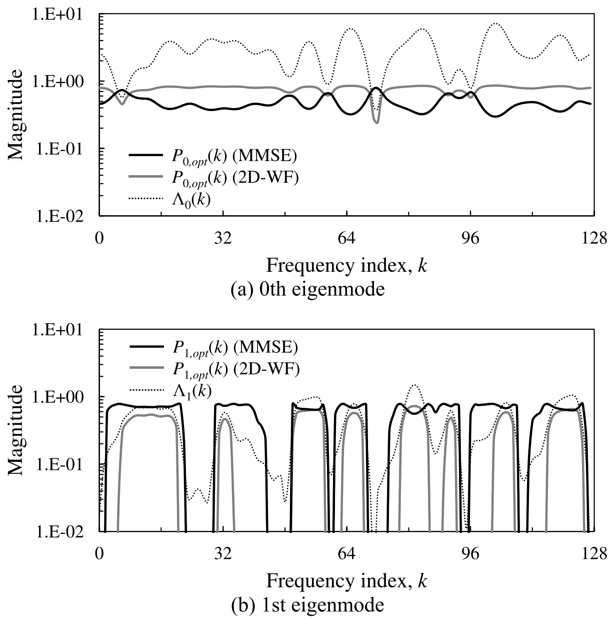

Fig. 2 One shot observation of the power allocation.

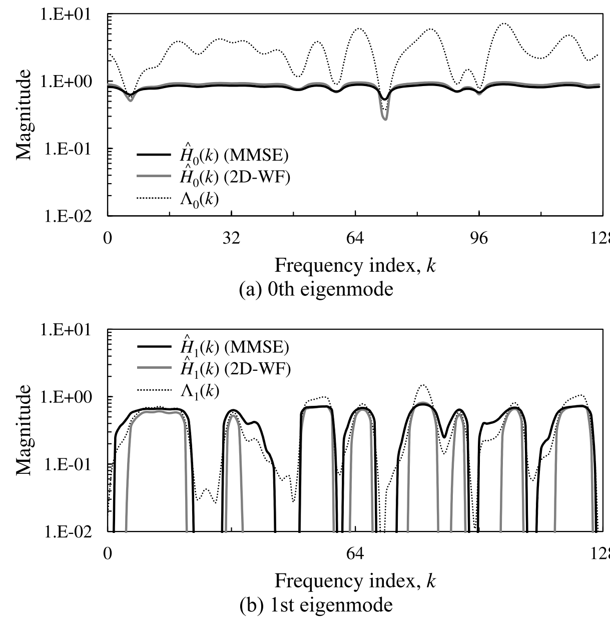

Fig. 3 One shot observation of the equivalent channel.

2.3 Discussion

In this section, we discuss the behavior of joint Tx/Rx MMSE filtering. The equivalent channel matrix $\hat{\mathbf{H}}(k)$ after the Rx MMSE filtering is expressed as

$$\begin{aligned}\hat{\mathbf{H}}(k) &= \mathbf{W}_{r,opt}(k)\mathbf{H}(k)\mathbf{W}_{t,opt}(k)\\ &= \mathrm{diag}\left[\begin{array}{l}\dfrac{P_{0,opt}(k)\Lambda_0(k)}{P_{0,opt}(k)\Lambda_0(k)+\gamma^{-1}},\ldots,\\ \dfrac{P_{G-1,opt}(k)\Lambda_{G-1}(k)}{P_{G-1,opt}(k)\Lambda_{G-1}(k)+\gamma^{-1}}\end{array}\right]\\ &\equiv \mathrm{diag}\left[\hat{H}_0(k),\ldots,\hat{H}_{G-1}(k)\right]. \end{aligned} \tag{15}$$

It can be seen from Eq. (15) that the MIMO channel matrix $\mathbf{H}(k)$ is diagonalized (i.e., the IAI is avoided) by joint Tx/Rx MMSE filtering. In addition, the ISI can be significantly suppressed by applying the MMSE based power allocation to each eigenmode following Eq. (14).

Figure 2 shows one shot observation of the proposed MMSE power allocation when $N_t = N_r = G = 2, N_c = 128, E_s/N_0 = 6$ dB, and a 16-path frequency-selective block Rayleigh fading having uniform power delay profile. It can be understood from Eq. (14) that the proposed MMSE power allocation is similar to the power allocation based on the well-known water-filling theory across both eigenmodes and frequencies (2D-WF) given as [2]

$$P_{g,opt}(k) = \max\left\{\frac{1}{\sqrt{\mu}} - \frac{1}{\gamma\Lambda_g(k)}, 0\right\}. \tag{16}$$

In Fig. 2, the conventional 2D-WF power allocation is also plotted for comparison. The 2D-WF power allocation is done by allocating much power to the eigenmodes and frequencies with high $\Lambda_g(k)$, and no power to those with low $\Lambda_g(k)$. Therefore, the ISI is enhanced and the transmission performance degrades. However, the proposed MMSE power allocation is quite different from the 2D-WF power allocation. In the proposed MMSE power allocation, each eigenmode and frequency has different threshold (first term of right side of Eq. (14)) because it depends on $\Lambda_g(k)$. Therefore, the proposed MMSE power allocation avoids the ISI enhancement by allocating power to the eigenmodes and frequencies which have comparatively low $\Lambda_g(k)$.

Figure 3 shows a one-shot observation of the equivalent channel $\hat{\mathbf{H}}(k)$ when the power allocation shown in Fig. 2 has been carried out. It can be seen from Fig. 3 that the ISI on the 0th eigenmode caused by the channel frequency-selectivity is sufficiently suppressed by the proposed MMSE power allocation and also by the 2D-WF power allocation. Since the ISI is not strong on the 0th eigenmode, the Rx MMSE filtering is enough to suppress the ISI. On the other hand, the ISI is stronger on the 1st eigenmode than on the 0th eigenmode. Therefore, the Rx MMSE filtering cannot sufficiently suppress the ISI on the 1st eigenmode. In fact, the received SINR of the 0th (1st) eigenmode is about 6.3 dB (−1.7 dB) when the proposed MMSE power allocation is used while that of the 0th (1st) eigenmode is about 7.9 dB (−4.5 dB) when the conventional 2D-WF power allocation is used. As a consequence, the proposed MMSE power allocation is effective to avoid the ISI enhancement on the 1st eigenmode but 2D-WF power allocation which does not consider the ISI is not.

3. Rank Adaptation and Adaptive Modulation

In this paper, to mitigate the degradation of transmission performance due to the received SINR gap among eigenmodes, we introduce rank adaptation and adaptive modulation to the SC-MIMO transmission. The number G of data streams (rank) and the modulation level for each eigenmode are jointly determined based on the minimum BER criterion. The transmission performance gap among eigenmodes can be narrowed by allocating no or a few bits (i.e., reducing the rank G or applying low level modulation) to the eigenmodes which have low received SINR and allocating many bits (i.e., applying high level modulation) to the eigenmodes which have high received SINR.

The received SINR Γ_g of the gth eigenmode in the proposed joint Tx/Rx MMSE filtering is given as (the derivation is shown in Appendix C)

$$\Gamma_g = \frac{\tilde{H}_g^2}{\frac{1}{N_c}\Sigma_{k=0}^{N_c-1}\hat{H}_g^2(k) - \tilde{H}_g^2 + \frac{\gamma^{-1}}{N_c}\Sigma_{k=0}^{N_c-1}\Sigma_{m=0}^{N_r-1}|W_{g,m}^{(r)}(k)|^2}, \tag{17}$$

where

$$\tilde{H}_g^2 = \frac{1}{N_c}\sum_{k=0}^{N_c-1}\hat{H}_g(k), \tag{18}$$

and $W_{g,m}^{(r)}(k)$ is the (g,m)th element of $\mathbf{W}_r(k)$.

When Gray code mapping is used and if ISI + noise can be approximated as a complex-valued random variable, the conditional BER $p_b^{(g)}$ of the gth eigenmode for the given set of modulation level and received SINR Γ_g is given as [4]

$$p_b^{(g)} = a_g \mathrm{erfc}\left(\sqrt{\frac{\Gamma_g}{b_g}}\right), \tag{19}$$

where erfc(.) denotes the complementary error function and a_g and b_g are shown in Table 1 for various modulation levels. When M_g bits are allocated to the symbol of the gth eigenmode, the conditional BER averaged over eigenmodes is given as

$$\bar{P}_b = \frac{\sum_{g=0}^{G-1} M_g p_b^{(g)}}{\sum_{g=0}^{G-1} M_g} = \frac{1}{\eta}\sum_{g=0}^{G-1} M_g a_g \mathrm{erfc}\left(\sqrt{\frac{\Gamma_g}{b_g}}\right), \tag{20}$$

where $\eta = \sum_{g=0}^{G-1} M_g$ is the spectral efficiency in bps/Hz.

The rank G and the modulation levels for G streams are jointly determined as follows. For the given spectral efficiency η, the average conditional BER is computed by using Eq. (20) for all possible combinations of G and modulation levels, and then, the optimal combination which minimizes the average conditional BER is found. For example, when $N_t = N_r = 2$ and $\eta = 4$(bps/Hz), possible combinations of G and modulation levels are $(G; M_0, M_1)$ = (1;4,0), (2;3,1), and (2;2,2), because $\Lambda_0(k)$ is always larger than $\Lambda_1(k)$ for $k = 0 \sim N_c - 1$. The average conditional BER is computed for the above 3 combinations to find the optimal one.

Table 1 a_g and b_g.

Data modulation	a_g	b_g
BPSK	1/2	1
QPSK	1/2	2
8PSK	1/3	$1/\sin^2(\pi/8)$
16QAM	3/8	10
64QAM	7/24	42
256QAM	15/64	170

4. Computer Simulation

4.1 Computer Simulation Condition

Computer simulation condition is summarized in Table 2. The channel is assumed to be a 16-path frequency-selective block Rayleigh fading having uniform power delay profile. Uncorrelated fading and ideal channel estimation at both the transmitter and receiver are also assumed.

4.2 Average BER Performance

Figure 4 shows the average BER performance of the proposed SC-MIMO transmission with joint Tx/Rx MMSE filtering (MMSE) and joint rank adaptation/adaptive modulation for $N_t = N_r = 4$ and $\eta = 16$ (bps/Hz). For comparison, the average BER performance of SC-MIMO transmission

Table 2 Computer simulation condition.

Parameter	Value
No. of DFT/IDFT points	N_c=128
Guard interval length	N_g=16
No. of Tx/Rx antennas	(N_t, N_r)=(4,4)
Fading	Frequency-selective block Rayleigh
Power delay profile	16-path uniform
Antenna correlation	Uncorrelated
Channel estimation	Ideal

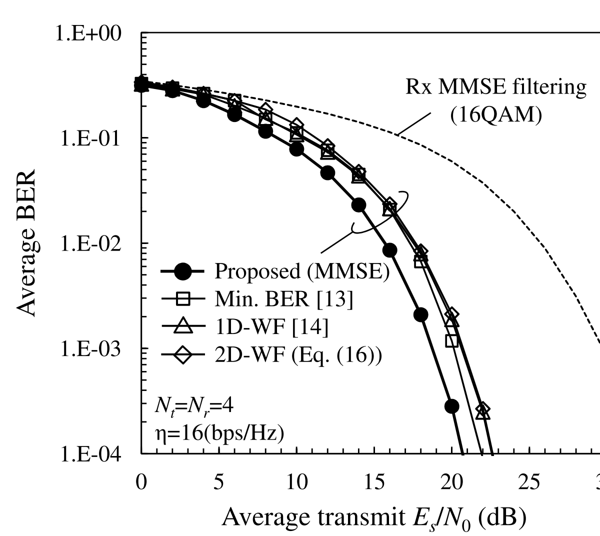

Fig. 4 Average BER performance.

using Rx MMSE filtering and the conventional eigenmode SC-MIMO transmissions with the minimum BER based power allocation (Min. BER) [13], the water-filling power allocation across eigenmode only (1D-WF) [14], and 2D-WF power allocation, are also plotted. 16QAM modulation is applied to N_t data streams when Rx MMSE filtering is used. The system models of the conventional eigenmode SC-MIMO transmissions with Min. BER, 1D-WF, and 2D-WF can be regarded as the same as Fig. 1 except for the power allocation in the "Tx MMSE filtering". Since the "Rx MMSE filtering" expressed as Eq. (7) considers the transmit filtering, any kind of power allocation can be used. It can be seen from Fig. 4 that the proposed SC-MIMO transmission with joint Tx/Rx MMSE filtering and joint rank adaptation/adaptive modulation achieves better average BER performance than SC-MIMO transmission using Rx MMSE filtering. For example, the proposed SC-MIMO transmission with joint Tx/Rx MMSE filtering and joint rank adaptation/adaptive modulation can reduce the required transmit E_s/N_0 to obtain the average BER = 10^{-3} about 10 dB compared to the SC-MIMO transmission using Rx MMSE filtering. This is because the proposed joint Tx/Rx filtering avoids the IAI by transforming the MIMO channel to eigenmodes and suppress the ISI by performing the MMSE power allocation shown in Fig. 2. In addition, a joint use of rank adaptation and adaptive modulation narrows the SINR gap between eigenmodes. The detailed discussion is given below.

The distribution of selected rank and modulation levels is shown in Fig. 5. It can be seen from Fig. 5 the probability that small G is selected and many bits are allocated to the eigenmodes which have high eigenvalues is high when average transmit E_s/N_0 is low. In the low average transmit E_s/N_0 region, the overall BER is improved by allocating the transmitted bits and applying high level modulation to the eigenmodes which have high eigenvalues (i.e., decreasing the rank G) because the received SINR of the eigenmode which have high eigenvalues are especially improved due to the high diversity gain. On the other hand, in the high average transmit E_s/N_0 region, the overall BER is improved by allocating the transmitted bits and applying low level modulation to multiple eigenmodes (i.e., increasing the rank G) because almost all of the eigenmodes have high received SINR.

Figure 4 shows that the proposed MMSE power allocation achieves the best average BER performance among MMSE, Min. BER, 1D-WF, 2D-WF. It is seen from Fig. 5 (a) that the rank G=3 is selected with a high probability when the average transmit E_s/N_0 is equal or larger than 6 dB using the proposed MMSE power allocation. This is because, as mentioned in Sect. 2.3, the proposed MMSE power allocation especially improves the SINRs of the eigenmodes which have low eigenvalues. Therefore, rank adaptation selects G=3 to allocate the transmitted bits to multiple eigenmodes and to apply low level modulations. Figures 5(b) and (c) show that the rank G=3 is also selected with a high probability when the average transmit E_s/N_0 is equal or larger

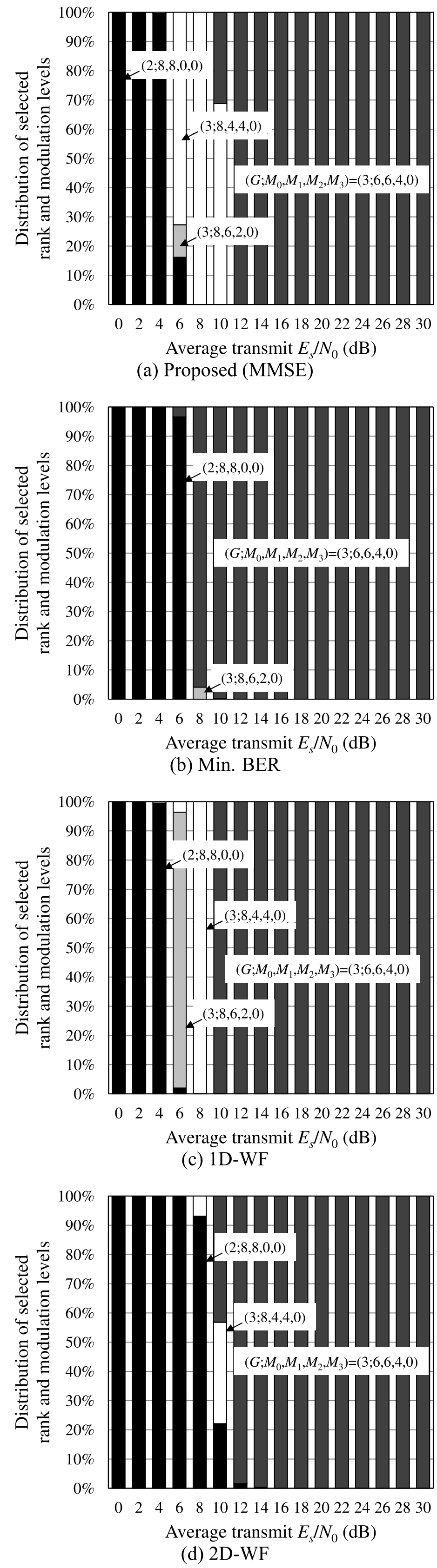

Fig. 5 Distribution of selected rank and modulation levels.

than 6 ∼ 8 dB using Min. BER and 1D-WF. However, they cannot suppress the ISI sufficiently because they perform equal power allocation across frequencies. As mentioned in Sect. 2.3, the ISI is enhanced and the received SINRs of the eigenmodes which have low eigenmodes especially degrade using 2D-WF. Therefore, G=2 and 256QAM are selected with a high probability when the average transmit E_s/N_0 is around 6 dB as shown in Fig. 5(d). As a result, the proposed MMSE power allocation achieves the best average BER performance.

5. Conclusion

In this paper, we proposed joint Tx/Rx MMSE filtering for SC-MIMO transmission. The proposed filtering avoids the IAI by transforming the MIMO channel to eigenmodes and at the same time, suppresses the ISI by performing MMSE power allocation. In addition, joint use of rank adaptation and adaptive modulation narrows the gap of received SINR among eigenmodes. Computer simulation confirmed that the proposed joint Tx/Rx MMSE filtering significantly improves the average BER performance and achieves better BER performance than the conventional eigenmode SC-MIMO transmission.

References

[1] E. Biglieri, R. Calderbank, A. Constantinides, A. Goldsmith, A. Paulraj, and H.V. Poor, MIMO Wireless Communications, Cambridge University Press, 2007.
[2] G.L. Stuber, J.R. Barry, S.W. Mclaughlin, Y. Li, M.A. Ingram, and T.G. Pratt, "Broadband MIMO-OFDM wireless communications," Proc. IEEE, vol.92, no.2, pp.271–294, Feb. 2004.
[3] Y. Lee, Y. You, W. Jeon, J. Paik, and H. Song, "Peak-to-average power ratio in MIMO-OFDM systems using selective mapping," IEEE Commun. Lett., vol.7, no.12, pp.575–577, Dec. 2003.
[4] J.G. Proakis and M. Salehi, Digital Communications, 5th ed., McGraw-Hill, 2008.
[5] S. Han and J. Lee, "An overview of peak-to-average power ratio reduction techniques for multicarrier transmission," IEEE Wireless Commun. Mag., vol.12, no.2, pp.56–65, April 2005.
[6] J.P. Coon and M.A. Beach, "An investigation of MIMO single-carrier frequency-domain MMSE equalization," London Communications Symposium, pp.237–240, 2002.
[7] S. Okuyama, T. Yamamoto, K. Takeda, and F. Adachi, "Iterative MMSE detection with interference cancellation for up-link HARQ using frequency-domain filtered SC-FDMA MIMO multiplexing," IEICE Trans. Commun., vol.E94-B, no.12, pp.3559–3568, Dec. 2011.
[8] K. Nagatomi, H. Kawai, and K. Higuchi, "Complexity-reduced MLD based on QR decomposition in OFDM MIMO multiplexing with frequency domain spreading and code multiplexing," EURASIP Journal on Advances in Signal Processing, vol.2011, no.5, pp.1–15, Jan. 2011.
[9] H. Sampath, P. Stoica, and A. Paulraj, "Generalized linear precoder and decoder design for MIMO channels using weighted MMSE criterion," IEEE Trans. Commun., vol.49, no.12, pp.2198–2206, Dec. 2001.
[10] K. Takeda and F. Adachi, "Joint transmit/receive one-tap mimimum mean square error frequency-domain equalisation for broadband multicode direct-sequence code division multiple access," IET Commun., vol.4, no.14, pp.1752–1764, Oct. 2010.
[11] D. Falconer, S.L. Ariyavisitakul, A. Benyamin-Seeyar, and B. Eidson, "Frequency domain equalization for single-carrier broadband wireless systems," IEEE Commun. Mag., vol.40, no.4, pp.58–66, April 2002.
[12] R.W. Heath, Jr. and A.J. Paulraj, "Switching between diversity and multiplexing in MIMO systems," IEEE Trans. Commun., vol.53, no.6, pp.962–968, June 2005.
[13] K. Miyashita, T. Nishimura, T. Ohgane, Y. Ogawa, Y. Takatori, and K. Cho, "High data-rate transmission with eigenbeam-space division multiplexing (E-SDM) in a MIMO channel," Proc. IEEE 56th Vehicular Technology Conference (VTC2002-Fall), pp.1302–1306, Vancouver, Canada, Sept. 2002.
[14] K. Ozaki, A. Nakajima, and F. Adachi, "Frequency-domain eigenmode-SDM and equalization for single-carrier transmissions," IEICE Trans. Commun., vol.E91-B, no.5, pp.1521–1530, May 2008.
[15] S. Boyd and L. Vandenberghe, Convex Optimization, Cambridge, 2006.
[16] R.A. Horn and C.R. Johnson, Matrix Analysis, Cambridge University Press, 1985.
[17] N. Ohkubo and T. Ohtsuki, "Design criteria for phase sequences in selected mapping," IEICE Trans. Commun., vol.E86-B, no.9, pp.2628–2636, Sept. 2003.

Appendix A: PAPR of Transmit Signal

PAPR of the transmit signal is defined as

$$\mathrm{PAPR} = \frac{\max\left\{|s_n(t)|^2\right\}}{E\left[|s_n(t)|^2\right]}, \tag{A·1}$$

$n = 0 \sim N_t - 1, t = 0, 1/8, \ldots, N_c - 1$. $\{s_n(t); t = 0, 1/8, \ldots, N_c - 1\}$ is the time-domain transmit signal waveform obtained by applying $8N_c$-point IDFT to $\{S_n(k); k = 0 \sim N_c - 1\}$. The PAPR is measured generating 8 times oversampled transmit signal waveforms. To evaluate the impact of $\mathbf{V}_t(k)$ to the PAPR of the transmit signal when $N_t = N_r = G = 2$, we consider four 2×2 unitary matrices as

$$\mathbf{V}_t^H(k) = \begin{cases} \begin{bmatrix} 1 & 0 \\ 0 & 1 \end{bmatrix} & \text{(identity matrix)} \\ \frac{1}{\sqrt{2}}\begin{bmatrix} 1 & 1 \\ 1 & -1 \end{bmatrix} & \text{(Walsh-Hadamard sequence)} \\ \frac{1}{\sqrt{2}}\begin{bmatrix} 1 & 1 \\ -1 & 1 \end{bmatrix} & \text{(Shapiro-Rudin sequence)} \\ \frac{1}{\sqrt{2}}\begin{bmatrix} 1 & j \\ j & 1 \end{bmatrix} & \text{(complex-valued matrix)} \end{cases} \tag{A·2}$$

Figure A·1 shows the complementary cumulative distribution function (CCDF) of the PAPR of SC-MIMO with Tx MMSE filtering when $N_c = 128$, $E_s/N_0 = 6$ dB, and a 16-path frequency-selective block Rayleigh fading having uniform power delay profile. 16QAM is applied to all eigenmodes and the same $\mathbf{V}_t(k)$ is used among all frequencies. For comparison, the CCDF of the PAPR of conventional SC-MIMO without Tx MMSE filtering and that of OFDM-MIMO are also shown in Fig. A·1. It is seen from Fig. A·1

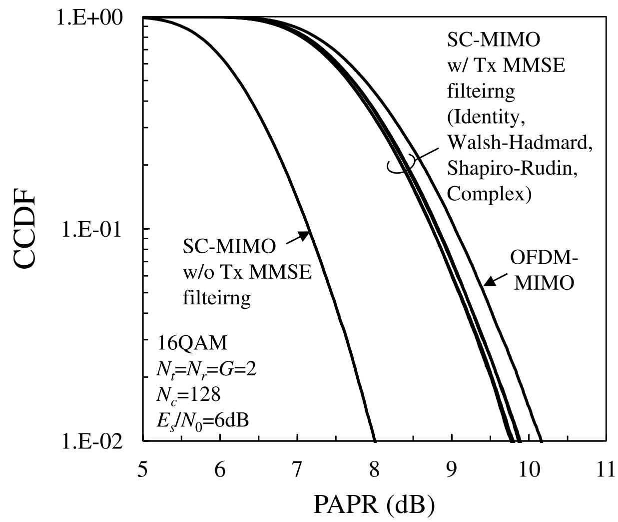

Fig. A· 1 CCDF of PAPR.

that the PAPR is increased by Tx MMSE filtering with any of the above $\mathbf{V}_t(k)$. This is because the phase of each component of the frequency-domain signal vector $\mathbf{D}(k)$ is rotated by $\mathbf{U}_t(k) = \mathbf{V}_h(k)$ in the transmit filter matrix $\mathbf{W}_t(k)$.

It is also seen from Fig. A· 1 that the choice of $\mathbf{V}_t(k)$ does not affect the PAPR performance. The PAPR increase caused by the phase rotation cannot be suppressed since the same $\mathbf{V}_t(k)$ is used at all frequencies in this paper. However, the PAPR can be reduced by introducing the concept of selected mapping [17] which has been proposed for PAPR reduction and selecting appropriate $\mathbf{V}_t(k)$ at each frequency. Introducing PAPR reduction technique is left as an interesting future study.

Appendix B: Derivation of Eq. (14)

To derive $P_{g,opt}(k)$; $g = 0 \sim G-1$, $k = 0 \sim N_c - 1$, the permutated index $v = 0 \sim GN_c - 1$ is introduced so that $\Lambda(0) \geq \ldots \Lambda(v) \geq \ldots \Lambda(GN_c-1)$. The optimization problem given by Eq. (13) can be rewritten as

$$P_{opt}(v) = \underset{\{P(v);v=0\sim GN_c-1\}}{\arg\min} \sum_{v=0}^{GN_c-1} \frac{1}{\gamma P(v)\Lambda(v)+1}$$
$$\text{s.t.} \begin{cases} \sum_{v=0}^{GN_c-1} P(v) = N_c \\ P(v) \geq 0 \text{ for } v = 0 \sim GN_c - 1. \end{cases} \quad \text{(A· 3)}$$

We assume that $P(v)$ has u non-zero elements and $(GN_c - u)$ zero elements $(0 \leq u \leq GN_c - 1)$, where u is determined so that the objective function is minimized. Since the objective function is a monotonically decreasing function of $P(v)$ for $v = 0 \sim GN_c - 1$, we have $P(v) \neq 0$ for $v = 0 \sim u - 1$ and $P(v) = 0$ for $v = u \sim GN_c - 1$. Eq. (A· 3) can be rewritten as

$$P_{opt}(v) = \underset{\{P(v);v=0\sim GN_c-1\}}{\arg\min} \sum_{v=0}^{GN_c-1} \frac{1}{\gamma P(v)\Lambda(v)+1}$$
$$\text{s.t.} \begin{cases} h_1 = \sum_{v=0}^{u-1} P(v) - N_c = 0 \\ h_2 = \sum_{v=u}^{GN_c-1} P(v) - 0 = 0 \\ f(P(v)) = -P(v) \leq 0 \text{ for } v = 0 \sim GN_c - 1. \end{cases} \quad \text{(A· 4)}$$

The optimization problem of Eq. (A· 4) can be solved by using the Lagrange multiplier method. The Lagrangian function L is expressed as [15]

$$L = \sum_{v=0}^{GN_c-1} \frac{1}{\gamma P(v)\Lambda(v)+1} + \mu h_1 + \kappa h_2 + \sum_{v=0}^{GN_c-1} \Psi(v) f(P(v)), \quad \text{(A· 5)}$$

where μ, κ, and $\Psi(v)$; $v = 0 \sim GN_c - 1$, are the Lagrange multipliers. The optimal solution $P_{opt}(v)$; $v = 0 \sim GN_c - 1$, must satisfy the KKT condition, and therefore, we obtain

$$\begin{cases} \left.\frac{\partial L}{\partial P(v)}\right|_{P_{opt}(v)} = 0 & \text{for } v = 0 \sim GN_c - 1 \\ \sum_{v=0}^{u-1} P_{opt}(v) - N_c = 0 & \\ \sum_{v=u}^{GN_c-1} P_{opt}(v) - 0 = 0 & \\ -P_{opt}(v) \leq 0 & \text{for } v = 0 \sim GN_c - 1 \\ \Psi(v) \geq 0 & \text{for } v = 0 \sim GN_c - 1 \\ \Psi(v) P_{opt}(v) = 0 & \text{for } v = 0 \sim GN_c - 1. \end{cases} \quad \text{(A· 6)}$$

Using Eqs. (A· 5) and (A· 6), we obtain

$$P_{opt}(v) = \max\left\{\frac{1}{\sqrt{\mu}} \frac{1}{\sqrt{\gamma\Lambda(v)}} - \frac{1}{\gamma\Lambda(v)}, 0\right\}, \quad \text{(A· 7)}$$

where

$$\frac{1}{\sqrt{\mu}} = \frac{N_c + \sum_{v=0}^{u-1} \frac{1}{\gamma\Lambda(v)}}{\sum_{v=0}^{u-1} \frac{1}{\sqrt{\gamma\Lambda(v)}}}. \quad \text{(A· 8)}$$

From Eq. (A· 7) and since v is the permutated index, $P_{g,opt}(k)$ can be derived as

$$P_{g,opt}(k) = \max\left\{\frac{1}{\sqrt{\mu}} \frac{1}{\sqrt{\gamma\Lambda_g(k)}} - \frac{1}{\gamma\Lambda_g(k)}, 0\right\}. \quad \text{(A· 9)}$$

Appendix C: Derivation of Eq. (17)

The $G \times 1$ frequency-domain soft-output vector $\hat{\mathbf{D}}(k)$ given by Eq. (3) can be rewritten by using Eq. (15) as

$$\hat{\mathbf{D}}(k) = \sqrt{\frac{2E_s}{T_s}} \hat{\mathbf{H}}(k)\mathbf{D}(k) + \mathbf{W}_r(k)\mathbf{Z}(k). \quad \text{(A· 10)}$$

Therefore, the gth frequency-domain soft-output signal $\hat{D}_g(k)$ is given as

$$\hat{D}_g(k) = \sqrt{\frac{2E_s}{T_s}} \hat{H}_g(k) D_g(k) + \sum_{m=0}^{N_r-1} W_{g,m}^{(r)}(k) Z_m(k). \quad \text{(A· 11)}$$

The gth time-domain soft-output signal $\hat{d}_g(t); g = 0 \sim G-1, t = 0 \sim N_c - 1$, after N_c-point IDFT is expressed as

$$\begin{aligned}\hat{d}_g(t) &= \frac{1}{\sqrt{N_c}} \sum_{k=0}^{N_c-1} \hat{D}_g(k) \exp(j2\pi kt/N_c) \\ &= \sqrt{\frac{2E_s}{T_s}} \tilde{H}_g d_g(t) + \xi_{\mathrm{ISI},g}(t) + \xi_{\mathrm{noise},g}(t), \qquad \text{(A· 12)}\end{aligned}$$

where $d_g(t); g = 0 \sim G-1,\ t = 0 \sim N_c - 1$, is the tth data-modulated symbol of the gth sequence expressed as

$$d_g(t) = \frac{1}{\sqrt{N_c}} \sum_{k=0}^{N_c-1} D_g(k) \exp(j2\pi kt/N_c). \qquad \text{(A· 13)}$$

$\xi_{\mathrm{ISI},g}(t)$ and $\xi_{\mathrm{noise},g}(t)$ are the residual ISI and equivalent noise, respectively, of the gth eigenmode after joint Tx/Rx MMSE filtering expressed as

$$\begin{cases} \xi_{\mathrm{ISI},g}(t) &= \sqrt{\frac{2E_s}{T_s}} \frac{1}{N_c} \sum_{k=0}^{N_c-1} \hat{H}_g(k) \\ & \quad \times \sum_{\substack{\tau=0 \\ \tau \neq t}}^{N_c-1} d_g(\tau) \exp\left(j2\pi k \frac{t-\tau}{N_c}\right) \\ \xi_{\mathrm{noise},g}(t) &= \frac{1}{N_c} \sum_{k=0}^{N_c-1} \sum_{m=0}^{N_r-1} W_{g,m}^{(r)}(k) Z_m(k) \\ & \quad \times \exp\left(j2\pi t \frac{k}{N_c}\right) \end{cases}. \qquad \text{(A· 14)}$$

Using Eq. (A· 14), the variance $2\sigma^2_{\mathrm{ISI},g}$ of $\xi_{\mathrm{ISI},g}(t)$ is given as

$$\begin{aligned} 2\sigma^2_{\mathrm{ISI},g} &= E\left[|\xi_{\mathrm{ISI},g}(t)|^2\right] \\ &= \frac{2E_s}{T_s} \frac{1}{N_c^2} \sum_{k=0}^{N_c-1} \sum_{k'=0}^{N_c-1} \hat{H}_g(k) \hat{H}_g(k') \\ & \times \sum_{\substack{\tau=0 \\ \tau \neq t}}^{N_c-1} \sum_{\substack{\tau'=0 \\ \tau' \neq t}}^{N_c-1} E\left[d_g(\tau) d_g^*(\tau')\right] \\ & \times \exp\left(j2\pi k \frac{t-\tau}{N_c}\right) \exp\left(j2\pi k \frac{t-\tau'}{N_c}\right). \qquad \text{(A· 15)} \end{aligned}$$

Since we assume $E[d_g(\tau) d_g^*(\tau')] = \delta(\tau - \tau')$, where $\delta(.)$ is the delta function, we have

$$\begin{aligned} 2\sigma^2_{\mathrm{ISI},g} &= \frac{2E_s}{T_s} \frac{1}{N_c^2} \sum_{k=0}^{N_c-1} \sum_{k'=0}^{N_c-1} \hat{H}_g(k) \hat{H}_g(k') \\ & \quad \times \sum_{\substack{\tau=0 \\ \tau \neq t}}^{N_c-1} \exp\left(j2\pi (k-k') \frac{t-\tau}{N_c}\right) \\ &= \frac{2E_s}{T_s} \frac{1}{N_c^2} \sum_{k=0}^{N_c-1} \sum_{k'=0}^{N_c-1} \hat{H}_g(k) \hat{H}_g(k') \\ & \quad \times (N_c \delta(k-k') - 1) \\ &= \frac{2E_s}{T_s} \left(\frac{1}{N_c} \sum_{k=0}^{N_c-1} \hat{H}_g^2(k) - \tilde{H}_g^2\right). \qquad \text{(A· 16)} \end{aligned}$$

As same as the case of residual ISI, the variance $2\sigma^2_{\mathrm{noise},g}$ of $\xi_{\mathrm{noise},g}(t)$ is given as

$$\begin{aligned} 2\sigma^2_{\mathrm{noise},g} &= E\left[|\xi_{\mathrm{noise},g}(t)|^2\right] \\ &= \frac{1}{N_c^2} \sum_{k=0}^{N_c-1} \sum_{k'=0}^{N_c-1} \sum_{m=0}^{N_r-1} \sum_{m'=0}^{N_r-1} W_{g,m}^{(r)}(k) \left(W_{g,m}^{(r)}(k)\right)^* \\ & \times E\left[Z_m(k) Z_{m'}^*(k')\right] \exp\left(j2\pi t \frac{k-k'}{N_c}\right). \qquad \text{(A· 17)} \end{aligned}$$

Since we assume $E[Z_m(k) Z_{m'}^*(k')] = (2N_c N_0/T_s)\delta(m-m')$, we have

$$\begin{aligned} 2\sigma^2_{\mathrm{noise},g} &= \frac{2N_0}{T_s} \frac{1}{N_c^2} \sum_{k=0}^{N_c-1} \sum_{k'=0}^{N_c-1} \sum_{m=0}^{N_r-1} W_{g,m}^{(r)}(k) \left(W_{g,m}^{(r)}(k)\right)^* \\ & \quad \times \exp\left(j2\pi t \frac{k-k'}{N_c}\right) \\ &= \frac{2N_0}{T_s} \frac{1}{N_c^2} \sum_{k=0}^{N_c-1} \sum_{m=0}^{N_r-1} |W_{g,m}^{(r)}(k)|^2. \end{aligned}$$

(A· 18)

From Eqs. (A· 12), (A· 16), and (A· 18), the received SINR Γ_g of the gth eigenmode in the proposed joint Tx/Rx MMSE filtering is given as

$$\Gamma_g = \frac{\tilde{H}_g^2}{\frac{1}{N_c} \sum_{k=0}^{N_c-1} \hat{H}_g^2(k) - \tilde{H}_g^2 + \frac{\gamma^{-1}}{N_c} \sum_{k=0}^{N_c-1} \sum_{m=0}^{N_r-1} |W_{g,m}^{(r)}(k)|^2}.$$

(A· 19)

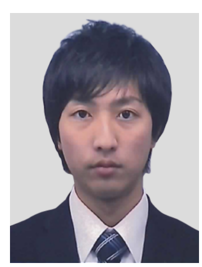

Shinya Kumagai received his B.E. degree in Information and Intelligent Systems in 2011 and M.E. degree in Electrical and Communications engineering in 2013, respectively, from Tohoku University, Sendai, Japan. Currently, he is a Japan Society for the Promotion of Science (JSPS) research fellow, studying toward his Ph.D. degree at the Department of Communications Engineering, Graduate School of Engineering, Tohoku University. His research interests include channel equalization and multiple-input multiple-output (MIMO) transmission techniques for mobile communication systems. He was a recipient of the 2012 IEICE RCS (Radio Communication Systems) Outstanding Research Award.

Tatsunori Obara received his B.S. degree in Electrical, Information and Physics Engineering in 2008 and M.S. and Dr. Eng. degrees in communications engineering, in 2010 and 2012, respectively, from Tohoku University, Sendai Japan. From April 2012 to March 2013, he was a Japan Society of the Promotion of Science (JSPS) research fellow at the Department of Communications Engineering, Graduate School of Engineering, Tohoku University. Since April 2013, he has been with NTT DOCOMO, Inc. His research interests include channel equalization and multiple-input multiple-output (MIMO) transmission techniques for mobile communication system.

Tetsuya Yamamoto received his B.S. degree in Electrical, Information and Physics Engineering in 2008 and M.S. and Dr. Eng. degrees in communications engineering from Tohoku University, Sendai Japan, in 2010 and 2012, respectively. From April 2010 to March 2013, he was a Japan Society for the Promotion of Science (JSPS) research fellow. Since April 2013, he has been with Panasonic Corporation. He was a recipient of the 2008 IEICE RCS (Radio Communication Systems) Active Research Award and Ericsson Best Student Award 2012.

Fumiyuki Adachi received the B.S. and Dr. Eng. degrees in electrical engineering from Tohoku University, Sendai, Japan, in 1973 and 1984, respectively. In April 1973, he joined the Electrical Communications Laboratories of Nippon Telegraph & Telephone Corporation (now NTT) and conducted various types of research related to digital cellular mobile communications. From July 1992 to December 1999, he was with NTT Mobile Communications Network, Inc. (now NTT DoCoMo, Inc.), where he led a research group on wideband/broadband CDMA wireless access for IMT-2000 and beyond. Since January 2000, he has been with Tohoku University, Sendai, Japan, where he is a Professor of Communications Engineering at the Graduate School of Engineering. In 2011, he was appointed a Distinguished Professor. His research interests are in the areas of wireless signal processing and networking including broadband wireless access, equalization, transmit/receive antenna diversity, MIMO, adaptive transmission, and channel coding, etc. From October 1984 to September 1985, he was a United Kingdom SERC Visiting Research Fellow in the Department of Electrical Engineering and Electronics at Liverpool University. Dr. Adachi is an IEEE fellow and a VTS Distinguished Lecturer for 2011 to 2013. He was a co-recipient of the IEEE Vehicular Technology Transactions best paper of the year award 1980 and again 1990 and also a recipient of Avant Garde award 2000. He was a recipient of Thomson Scientific Research Front Award 2004 and Ericsson Telecommunications Award 2008, Telecom System Technology Award 2009, and Prime Minister Invention Prize 2010.